We are IntechOpen, the world's leading publisher of Open Access books Built by scientists, for scientists

4,800
Open access books available

122,000
International authors and editors

135M
Downloads

Our authors are among the

154
Countries delivered to

TOP 1%
most cited scientists

12.2%
Contributors from top 500 universities

CLARIVATE ANALYTICS BOOK CITATION INDEX INDEXED

WEB OF SCIENCE™

Selection of our books indexed in the Book Citation Index in Web of Science™ Core Collection (BKCI)

Interested in publishing with us?
Contact book.department@intechopen.com

Numbers displayed above are based on latest data collected.
For more information visit www.intechopen.com

2

Array Processing: Underwater Acoustic Source Localization

Salah Bourennane, Caroline Fossati and Julien Marot
Institut Fresnel, Ecole Centrale Marseille
France

1. Introduction

Array processing is used in diverse areas such as radar, sonar, communications and seismic exploration. Usually the parameters of interest are the directions of arrival of the radiating sources. The High-Resolution subspace-based methods for direction-of-arrival (DOA) estimation have been a topic of great interest. The subspace-based methods well-developed so far require a fundamental assumption, which is that the background noise is uncorrelated from sensor to sensor, or known to within a multiplicative scalar. In practice this assumption is rarely fulfilled and the noise received by the array may be a combination of multiple noise sources such as flow noise, traffic noise, or ambient noise, which is often correlated along the array (Reilly & Wong, 1992; Wu & Wong, 1994). However, the spatial noise is estimated by measuring the spectrum of the received data when no signal is present. The data for parameter estimation is then pre-whitened using the measured noise. The problem with this method is that the actual noise covariance matrix varies as a function of time in many applications. At low signal-to-noise ratio (SNR) the deviations from the assumed noise characteristics are critical and the degradation may be severe for the localization result. In this chapter, we present an algorithm to estimate the noise with band covariance matrix. This algorithm is based on the noise subspace spanned by the eigenvectors associated with the smallest eigenvalues of the covariance matrix of the recorded data. The goal of this study is to investigate how perturbations in the assumed noise covariance matrix affect the accuracy of the narrow-band signal DOA estimates (Stoica et al., 1994). A maximum likelihood algorithm is presented in (Wax, 1991), where the spatial noise covariance is modeled as a function of certain unknown parameters. Also in (Ye & DeGroat, 1995) a maximum likelihood estimator is analyzed. The problem of incomplete pre-whitening or colored noise is circumvented by modeling the noise with a simple descriptive model. There are other approaches to the problem of spatially correlated noise: one is based on the assumption that the correlation structure of the noise field is invariant under a rotation or a translation of the array, while another is based on a certain linear transformation of the sensor output vectors (Zhang & Ye, 2008; Tayem et al., 2006). These methods do not require the estimation of the noise correlation function, but they may be quite sensitive to the deviations from the invariance assumption made, and they are not applicable when the signals also satisfy the invariance assumption.

2. Problem formulation

Consider an array of N sensors which receive the signals in one wave field generated by P $(P < N)$ sources in the presence of an additive noise. The received signal vector is sampled

and the DFT algorithm is used to transform the data into the frequency domain. We represent these samples by:

$$\mathbf{r}(f) = \mathbf{A}(f)\mathbf{s}(f) + \mathbf{n}(f) \tag{1}$$

where $\mathbf{r}(f)$, $\mathbf{s}(f)$ and $\mathbf{n}(f)$ are respectively the Fourier transforms of the array outputs, the source signals and the noise vectors. The $\mathbf{A}(f)$, matrix of dimensions $(N \times P)$ is the transfer matrix of the source-sensor array systems with respect to some chosen reference point. The sensor noise is assumed to be independent of the source signals and partially spatially correlated. The sources are assumed to be uncorrelated. The covariance matrix of the data can be defined by the $(N \times N)$-dimensional matrix.

$$\mathbf{\Gamma}(f) = E[\mathbf{r}(f)\mathbf{r}^{+}(f)] \tag{2}$$

$$\mathbf{\Gamma}(f) = \mathbf{A}(f)\mathbf{\Gamma}_s(f)\mathbf{A}^{+}(f) + \mathbf{\Gamma}_n(f) \tag{3}$$

Where $E[.]$ denotes the expectation operator, superscript $+$ represents conjugate transpose, $\mathbf{\Gamma}_n(f) = E[\mathbf{n}(f)\mathbf{n}^{+}(f)]$ is the $(N \times N)$ noise covariance matrix, and $\mathbf{\Gamma}_s(f) = E[\mathbf{s}(f)\mathbf{s}^{+}(f)]$ is the $(P \times P)$ signal covariance matrix. The above assumption concerning the non-correlation of the sources means that $\mathbf{\Gamma}_s(f)$ is full rank.

The High-Resolution algorithms of array processing assume that the matrix $\mathbf{\Gamma}_n(f)$ is diagonal. The subspace-based techniques are based on these properties. For example the MUSIC (Multiple Signal Classification)(Cadzow, 1998) null-spectrum $P_{music}(\theta)$ is defined by :

$$P_{music}(\theta) = \frac{1}{|\mathbf{a}^{+}(\theta)\hat{\mathbf{V}}_N(f)\hat{\mathbf{V}}_N^{+}(f)\mathbf{a}(\theta)|} \tag{4}$$

and it is expected that $P_{music}(\theta)$ has maximum points around $\theta \in \{\theta_1, ..., \theta_P\}$, where $\theta_1, ..., \theta_p$ are the directions of arrival of the sources and $\hat{\mathbf{V}}_N(f) = \{\mathbf{v}_{P+1}(f) \dots \mathbf{v}_N(f)\}$. Therefore, we can estimate the DOA by taking the local maximum points of $P_{music}(\theta)$.

In this chapter, we consider that the matrix $\mathbf{\Gamma}_n(f)$ is not diagonal because the noise realizations are spatially correlated and then the performances of these methods are considerably degraded.

3. Modeling the noise field

A fundamental limitation of the standard parametric array processing algorithms is that the covariance matrix of background noise cannot, in general, be estimated along with the signal parameters. So this leads to an unidentifiable parametrization, the measured data should always be regarded to consist of only the noise with a covariance matrix equal to that of the observed sample. This is a reason for imposing a model on the background noise. Several parametric noise models have been proposed in some literatures recently. Here, as well as in (Zhang & Ye, 2008), a descriptive model will be used, that is, the spatial noise covariance matrix is assumed to consist of a linear combination of some unknown parameters, which are weighted by known basis matrices. There are two different noise phenomenons to be described. We can model the noise as:

- an internal noise generated by the sensors so-called thermal noise. This noise is assumed to be independent (Zhang & Ye, 2008; Werner & Jansson, 2007) from sensor to sensor, but not necessarily spatially white. Then the spatial covariance matrix of this noise denoted $\mathbf{\Gamma}_n^S(f)$ is diagonal.

- an external noise received on the sensors, whose spatial covariance matrix is assumed to have the following structure (Zhang & Ye, 2008; Werner & Jansson, 2007; Friedlander & Weiss, 1995), $\mathbf{\Gamma}_n^B(f) = \sum_{k=1}^{K} \alpha_k \beta_k$, where α_k are unknown parameters and β_k are complex weighting matrices, β_k are chosen such that $\mathbf{\Gamma}_n^B(f)$ is positive definite and of band structure.

Consequently, the additive noise is the sum of these two noise terms and the spatial covariance matrix is

$$\mathbf{\Gamma}_n(f) = \mathbf{\Gamma}_n^S(f) + \mathbf{\Gamma}_n^B(f) \tag{5}$$

4. Modeling the covariance matrix of the band noise

In many applications when a uniform linear array antenna system is used, it is reasonable to assume that noise correlation is decreasing along the array (see Fig. 1). This is a widely used model for colored noise. We can then obtain a specific model for noise correlation under the following assumptions:

- the correlation length is K which means that the spatial correlation attains up to the $K-$th sensor;
- the noise realizations received by sensors which are separated with a distance no less than Kd, where d is the distance between sensors, are considered uncorrelated,

The noise correlation model which is obtained is represented on Fig. 1.

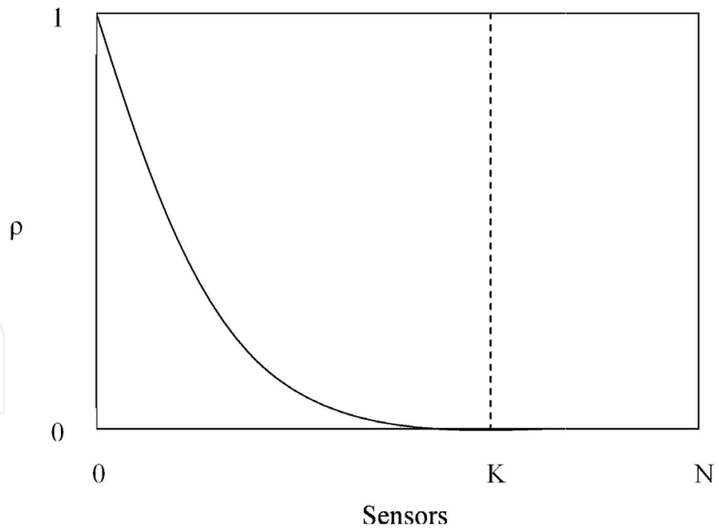

Fig. 1. Noise correlation along an uniform linear array with N sensors, ρ is the noise spatial correlation coefficient.

In this chapter the noise covariance matrix is modeled as an Hermitian, positive-definite band matrix $\Gamma_n(f)$, with half-bandwidth K. The $(i,m)-$th element of $\Gamma_n(f)$ is ρ_{mi} with:

$$\rho_{mi} = 0, \qquad for \qquad |i-m| \geq K \qquad i,m = 1,\ldots,N$$

$$\Gamma_n = \begin{pmatrix} \sigma_1^2(f) & \rho_{12}(f) & \cdots \\ \rho_{12}^*(f) & \sigma_2^2(f) & \cdots \\ \vdots & \ddots & \ddots \\ \rho_{1K}^*(f) & \cdots & \rho_{K-1}^*(f) \\ \vdots & \ddots & \ddots \\ 0 & \cdots & \rho_{KN}^*(f) \\ \rho_{1K}(f) & \cdots & 0 \\ \rho_{1(K+1)}(f) & \cdots & 0 \\ \cdots & \ddots & \vdots \\ \sigma_K^2(f) & \cdots & \rho_{KN}(f) \\ \cdots & \ddots & \vdots \\ \cdots & \rho_{K(N-1)}^*(f) & \sigma_N^2(f) \end{pmatrix}$$

Where $\rho_{mi} = \bar{\rho}_{mi} + j\tilde{\rho}_{mi}$; i,m=1,...,N; ρ_{mi} are complex variables, $j^2 = -1$ and σ_i^2 is the noise variance at the ith sensor, and $*$ denotes complex conjugate.
In the following section, an algorithm to estimate the band noise covariance matrix is developed for narrow-band signals.

5. Estimation of the noise covariance matrix

5.1 Proposed algorithm

Several methods have been proposed for estimating the directions of arrival of multiple sources in unknown noise fields. Initially the noise spectral matrix is measured, when signals of interest are not present. Other techniques (Abeidaa & Delmas, 2007) based on the maximum likelihood algorithm are developed, which incorporate a noise model to reduce the bias for estimating both the noise covariance matrix and the directions of arrival of the sources.

Our approach is realized in two steps. Using an iterative algorithm, the noise covariance matrix is estimated, then this estimate is subtracted from the covariance matrix of the received signals.

The proposed algorithm for estimating the noise covariance matrix can be summarized as follows:

Step 1 : Estimate the covariance matrix $\Gamma(f)$ of the received signals by the expectation of T time measures noted by $\hat{\Gamma}(f)$. $\hat{\Gamma}(f) = \frac{1}{T}\left[\sum_{t=1}^{T} \mathbf{r_t}(\mathbf{f})\mathbf{r_t^+}(\mathbf{f})\right]$. The eigendecomposition of this matrix is given by:

$\hat{\Gamma}(f) = \mathbf{V}(f)\Lambda(f)\mathbf{V}^+(f)$ with $\Lambda(f) = diag[\lambda_1(f),...,\lambda_N(f)]$ and $\mathbf{V}(f) = [\mathbf{v}_1(f),\mathbf{v}_2(f),...,\mathbf{v}_N(f)]$ where $\lambda_i(f), i = 1...N, (\lambda_1 \geq \lambda_2 \geq,...,\geq \lambda_N)$, and $\mathbf{v}_i(f)$ are respectively the i-th eigenvalue and the corresponding eigenvector.

And we initialize the noise covariance matrix by $\Gamma_n^0(f) = \mathbf{0}$.

Step 2 : Calculate $\mathbf{W}_P = \mathbf{V}_S(f)\Lambda_S^{1/2}(f)$, and $\mathbf{V}_S(f) = [\mathbf{v}_1(f),\mathbf{v}_2(f),...,\mathbf{v}_P(f)]$ is the matrix of the P eigenvectors associated with the first P largest eigenvalues of $\hat{\Gamma}(f)$.
Let $\Delta^1 = \mathbf{W}_P(f)\mathbf{W}_P^+(f)$.

Step 3 : Calculate the (i, j)th element of the current noise covariance matrix

$$[\Gamma_n^1(f)]_{ij} = [\hat{\Gamma}(f) - \Delta^1]_{ij} \quad if \ \ | \ i-j \ | < K \ \ i,j = 1, ..., N$$

and

$$[\Gamma_n^1(f)]_{ij} = 0 \quad if \ \ | \ i-j \ | \geq K$$

$$\Gamma_n^l(f) = \begin{pmatrix} \Gamma_{11}^l(f) - \Delta_{11}^l(f) & \cdots & \Gamma_{1K}^l(f) - \Delta_{1K}^l(f) \\ \vdots & \ddots & \ddots \\ \Gamma_{K1}^l(f) - \Delta_{K1}^l(f) & \cdots & \Gamma_{KK}^l(f) - \Delta_{KK}^l(f) \\ \vdots & \ddots & \ddots \\ 0 & \cdots & \cdots \\ \cdots & 0 & \\ \cdots & \vdots & \\ \cdots & \Gamma_{NK}^l(f) - \Delta_{NK}^l(f) & \\ \cdots & \vdots & \\ \cdots & \Gamma_{NN}^l(f) - \Delta_{NN}^l(f) & \end{pmatrix}$$

Step 4 : Eigendecomposition of the matrix $[\hat{\Gamma}(f) - \Gamma_n^1(f)]$. The new matrices $\Delta^2(f)$ and $\Gamma_n^2(f)$ are calculated using the previous steps. Repeat the algorithm until a significant improvement of the estimated noise covariance matrix is obtained.

Stop test : The iteration is stopped when $\|\Gamma_n^{l+1}(f) - \Gamma_n^l(f)\|_F < \epsilon$ with ϵ a fixed threshold. The difference between the Frobenius norms of matrices $\Gamma_n^{l+1}(f)$ and $\Gamma_n^l(f)$ is given by :

$$\|\Gamma_n^{l+1}(f) - \Gamma_n^l(f)\|_F = \Big[\sum_{i,j=1}^{N} t_{ij}^2(f) \Big]^{1/2}$$

where $t_{ij}(f) = [\Gamma_n^{l+1}(f) - \Gamma_n^l(f)]_{ij}$.

5.2 Spatial correlation length

In the previously proposed iterative algorithm, the spatial correlation length of the noise is supposed to be known. In practice, this is aforehand uncertain, therefore the search for a criterion of an estimate of K is necessary. In (Tayem et al., 2006), one algorithm which jointly estimates the number of sources and the spatial correlation length of the noise is presented. We propose to vary the value of K until the stability of the result is reached, that is, until the noise covariance matrix does not vary when K varies. The algorithm incorporating the choice of the correlation length K is presented in Fig. 2. In the stop test, we check whether $\|[\Gamma_n^{K+1}]_1(f) - [\Gamma_n^K]_1(f)\|_F < \epsilon$ or not.

6. Simulation results

In the following simulations, a uniform linear array of $N = 10$ omnidirectional sensors with equal inter-element spacing $d = \frac{c}{4f_o}$ is used, where f_o is the mid-band frequency and c is the velocity of propagation. The number of independent realizations used for estimating the

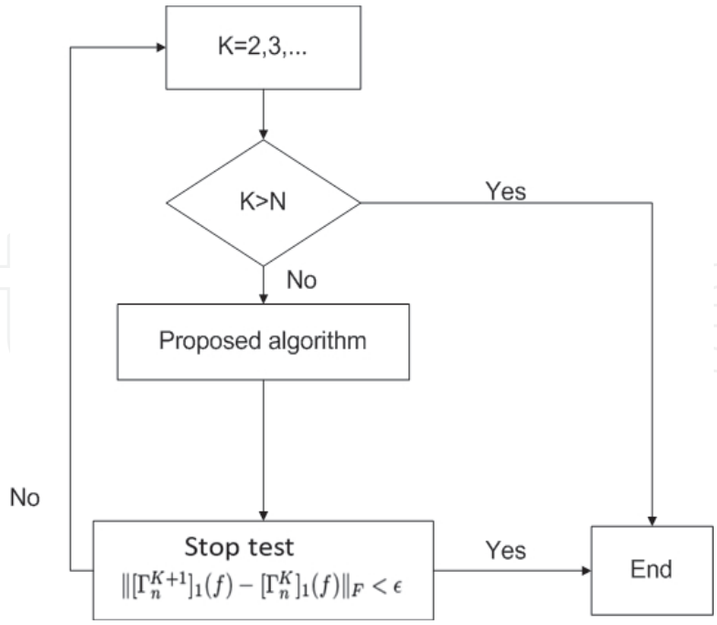

Fig. 2. Integration of the choice of K in the algorithm, where $[\Gamma_n^K]_1(f)$ indicates the principal diagonal of the banded noise covariance matrix $\Gamma_n(f)$ with spatial correlation length K.

covariance matrix of the received signals is 1000. The signal sources are temporally stationary zero-mean white Gaussian processes with the same frequency $f_o = 115\ Hz$. Three equi-power uncorrelated sources impinge on the array from different angles with the $SNR = 10dB$. The noise power is taken as the average of the diagonal elements of the noise covariance matrix $\sigma^2 = \frac{1}{N}\sum_{i=1}^{N}\sigma_i^2$.

To demonstrate the performance of the proposed algorithm, three situations are considered:

- Band-Toeplitz noise covariance matrix, with each element given by a modeling function;

- Band-Toeplitz noise covariance matrix, where the element values are arbitrary;

- Band noise covariance matrix, with each element arbitrary.

In each case, two spatial correlation lengths are studied: $K = 3$ and $K = 5$.

6.1 Noise covariance matrix estimation and results obtained

To localize the directions of arrival of sources and to evaluate the performance of the proposed algorithm, the High-Resolution methods such as MUSIC (Kushki & Plataniotis, 2009; Hawkes & Nehorai, 2001) are used after the preprocessing, with the exact number of sources ($P = 3$). This detection problem is not considered in this study.

Example 1 : *Band-Toeplitz noise covariance matrix:*

In this example, the spatial correlation between the noises is exponentially decreasing along the array of antenna and the elements of the noise covariance matrix are expressed as:

$$[\Gamma_n(f)]_{i,m} = \sigma^2\rho^{|i-m|}e^{j\pi(i-m)/2} \quad if \quad |i-m| < K$$

and,

$$[\Gamma_n(f)]_{i,m} = 0 \qquad if \quad |i-m| \geq K$$

where σ^2 is the noise variance equal for every sensor and ρ is the spatial correlation coefficient. The values which are retained are: $\sigma^2 = 1$ and $\rho = 0.7$.

In each of the two studied cases ($K = 3$ and $K = 5$), the noise covariance matrix is estimated with a fixed threshold value $\epsilon = 10^{-5}$ after a few iterations and we notice that the number of iterations for $K = 5$ is greater than that of $K = 3$.

Example 2 : *Band-Toeplitz noise covariance matrix*

In this example, the covariance matrix elements are chosen such that their values are decreasing along the array of antenna. The noise covariance matrix has the same structure as in example 1:

$$\Gamma_n = \begin{pmatrix} \sigma^2 & \rho_2 & \cdots & \rho_K & \cdots & 0 \\ \rho_2^* & \sigma^2 & \rho_2 & \cdots & \cdots & 0 \\ \vdots & \ddots & \ddots & \ddots & \ddots & \vdots \\ \rho_K^* & \ddots & \ddots & \ddots & \ddots & \vdots \\ \vdots & \ddots & \ddots & \ddots & \ddots & \vdots \\ 0 & \cdots & \rho_K^* & \cdots & \rho_2^* & \sigma^2 \end{pmatrix}$$

The parameters used are: in the case of $K = 3$, $\sigma^2 = 1$, $\rho_2 = 0.4 + 0.3j$ and $\rho_3 = 0.1 + 0.07j$. Using the proposed algorithm, the three complex parameters of the noise covariance matrix can be perfectly estimated.

- For $K = 5$: $\sigma^2 = 1$, $\rho_2 = 0.4 + 0.3j$, $\rho_3 = 0.1 + 0.07j$, $\rho_4 = 0.07 + 0.05j$ and $\rho_5 = 0.01 + 0.009j$. The proposed algorithm gives good estimates of the simulated parameters.

Example 3 : *Band noise covariance matrix with random elements:*

Each element of the band noise covariance matrix is obtained by the average of several simulations simulated with random numbers uniformly distributed in the interval (0,1).

For $K = 3$, Fig. 3 shows the differences between the 10 elements of the principal diagonal of the simulated matrix and those of the estimated matrix.

For $K = 5$, Fig. 4 shows the obtained results. Comparing these two results, we can remark that when K increases the estimation error increases. This concluding remark is observed on many simulations.

Figures 5, 6, 7, 8, 9 and 10 show the localization results of three sources before and after the preprocessing. Before the preprocessing, we use directly the MUSIC method to localize the sources. Once the noise covariance matrix is estimated with the proposed algorithm, this matrix is subtracted from the initial covariance matrix of the received signals, and then we use the MUSIC method to localize the sources. The three simulated sources are 5°, 10° and 20° for Fig. 5 and 6; 5°, 15° and 20° for Figs. 7 and 8; 5°, 15° and 25° for Fig. 9 and 10. For Figs. 7 and 8, the simulated SNR is greater than those of Figs. 5, 6 and Figs. 7 and 8.

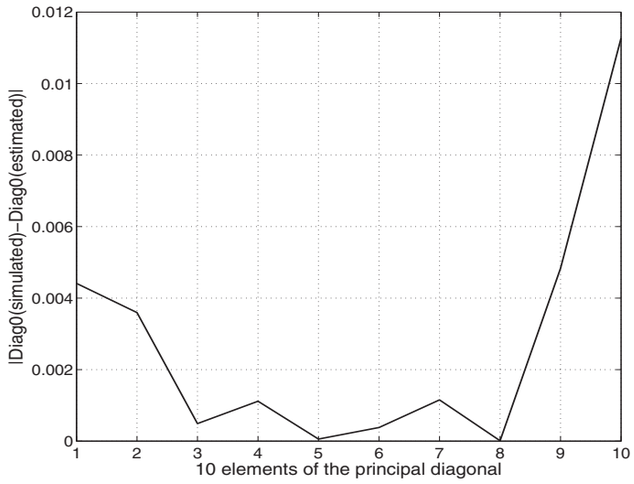

Fig. 3. Variations of the estimation error along the principal diagonal of the noise covariance matrix for $K = 3$.

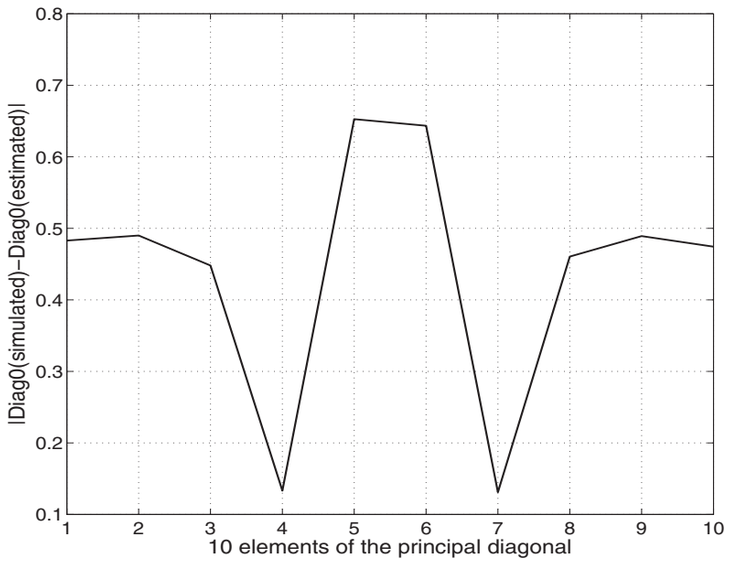

Fig. 4. Variations of the estimation error along the principal diagonal of the noise covariance matrix for $K = 5$.

The comparison of the results of Figs. 5, 6 and 7, 8 comes to the conclusion that the MUSIC method cannot separate the close sources without the preprocessing when the SNR is low, so in Fig. 5 we can only detect two sources before preprocessing. And for each case we can note that there is improvement in the results obtained with the preprocessing. Comparing the results of $K = 3$ with that of $K = 5$ for each figure, we can also reconfirm that when K increases, the estimation error increases on whitening, so we obtain better results with the preprocessing for $K = 3$ than $K = 5$.

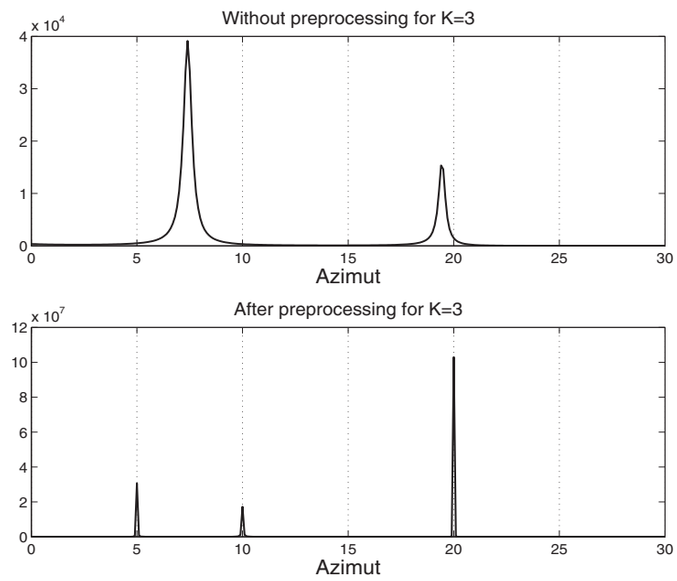

Fig. 5. Localization of the three sources at 5°, 10° and 20° without and with noise pre-processing for $K = 3$.

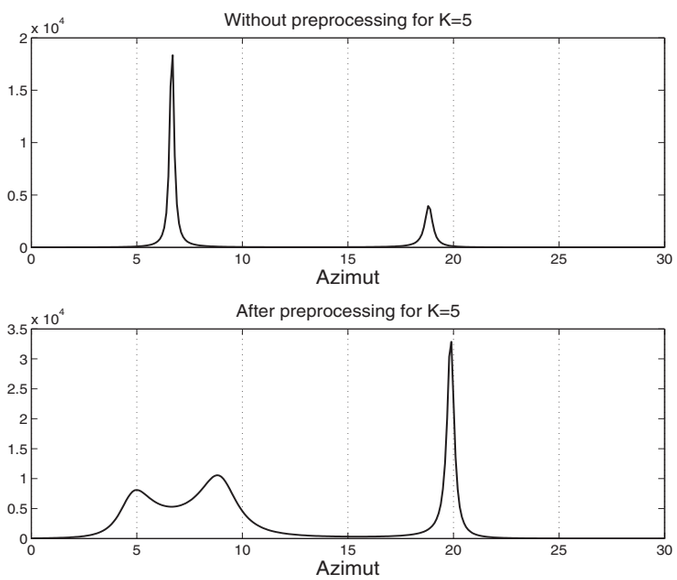

Fig. 6. Localization of the three sources at 5°, 10° and 20° without and with noise pre-processing for $K = 5$.

In order to evaluate the performances of this algorithm, we study, below, the influence of the involved parameters.

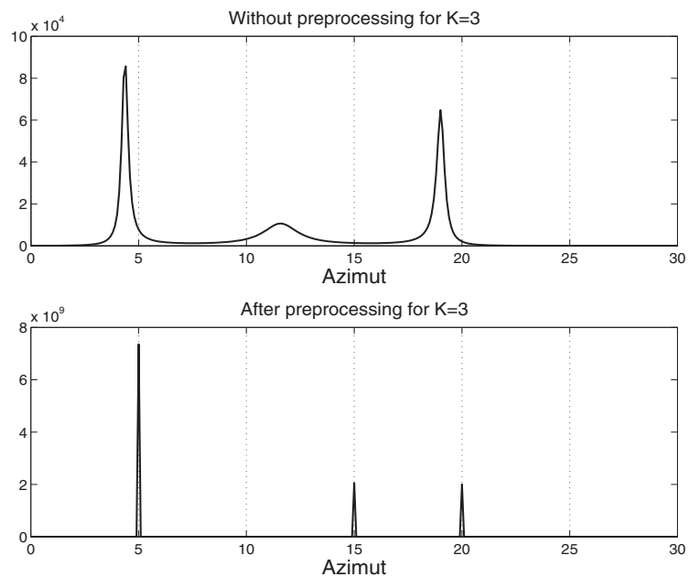

Fig. 7. Localization of the three sources at 5°, 15° and 20° without and with noise pre-processing with greater SNR than figure 5 for $K = 3$.

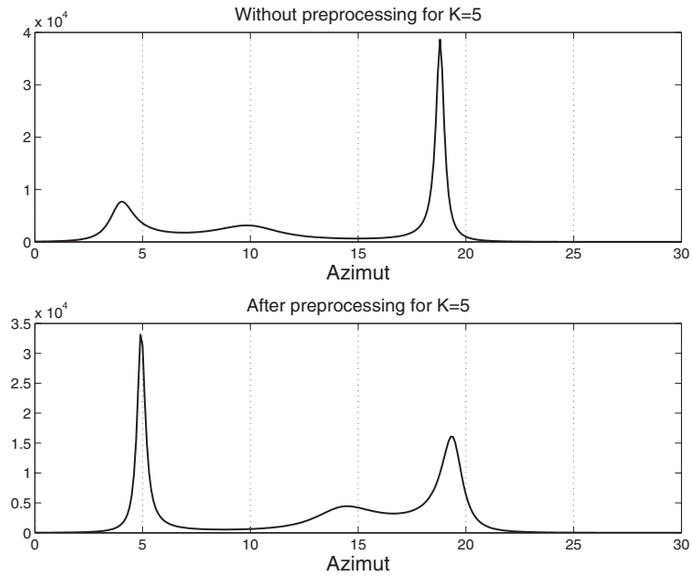

Fig. 8. Localization of the three sources at 5°, 15° and 20° without and with noise pre-processing with greater SNR than figure 6 for $K = 5$.

6.2 Choice of the parameters

6.2.1 Spatial correlation length of the noise

Figure 11 shows the variations of the estimation error of the noise covariance matrix when the spatial correlation length of the noise K is increasing from 2 to N and the number of sources is

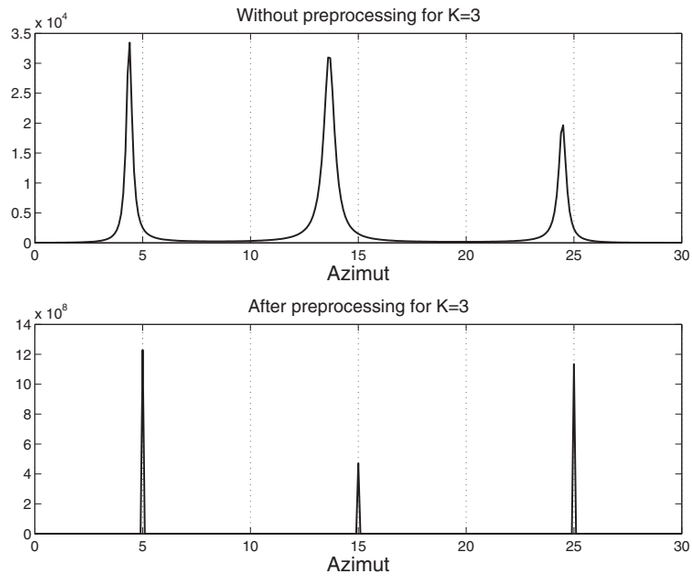

Fig. 9. Localization of the three sources at 5°, 15° and 25° without and with noise pre-processing for $K = 3$.

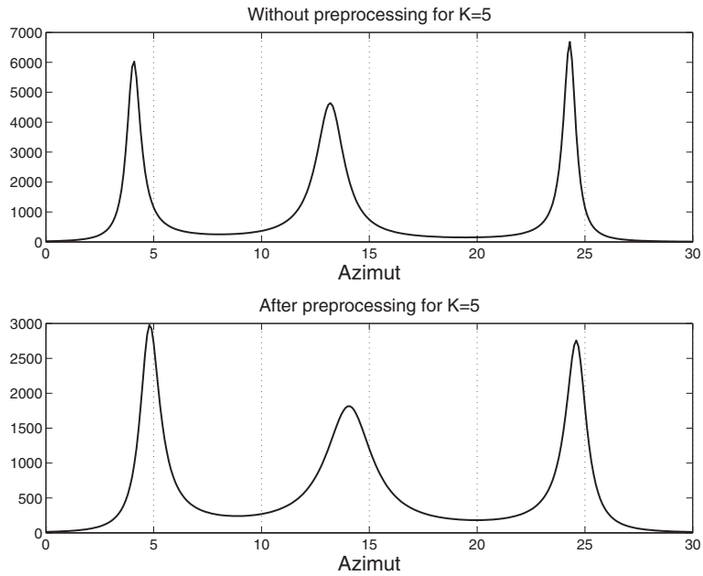

Fig. 10. Localization of the three sources at 5°, 15° and 25° without and with noise pre-processing for $K = 5$.

fixed to be P, $P = 1$ or $P = 9$. This error is defined by: $EE = \|\Gamma_n^{simulated} - \Gamma_n^{estimated}\|_F$.

Figure 11 shows that if $P = 1$, the estimation error is null until $K = 5$. On the other hand for $P = 9$, we have an estimation error of the covariance matrix of the noise as soon as $K = 2$ and the error is greater than the error for $P = 1$.

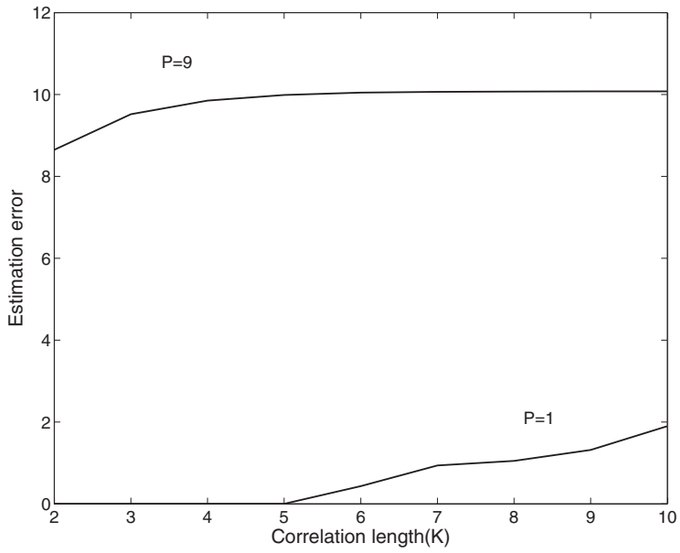

Fig. 11. Estimation error of the covariance matrix of the noise according to its spatial correlation length with P=1 and P=9.

To study the influence of K on the localization, we draw, Fig. 12, according to the spatial correlation length K of the noise, the variations of the bias of estimate of the azimuth in the case of only one source localized at 10°.

We define that the bias of the P estimated directions of the arrival of the sources is calculated by:

$$Bias = \frac{1}{P}\sum_{p=1}^{P} bias(p)$$

where

$$bias(p) = E\left[\theta(p) - \hat{\theta}(p)\right] = \frac{1}{T}\sum_{i=1}^{T} |\theta(i) - \hat{\theta}(i)|$$

The experimental results presented in Figs. 11 and 12 show that the correlation length and the number of sources influence the estimate of the covariance matrix of the noise and then the estimate of the DOA values. We study, below, the influence of the signal-to-noise ratio SNR on the estimate of the covariance matrix of the noise.

6.2.2 Signal-to-noise ratio influence

In order to study the performances of the proposed algorithm according to the signal-to-noise ratio, we plot, Fig. 13, the estimation error over the noise covariance matrix (the estimation error is defined in the section 6.2.1) according to the spatial correlation length K for $SNR = 0\ dB$ and $SNR = 10\ dB$.

We conclude that the choice of the value of K influences the speed and the efficiency of this algorithm. Indeed, many simulations show that this algorithm estimates the matrix quickly, if $K \ll N$. On the other hand if K is close to N, the algorithm requires a great number of iterations. This is due to the increase of the number of unknown factors to estimate. The

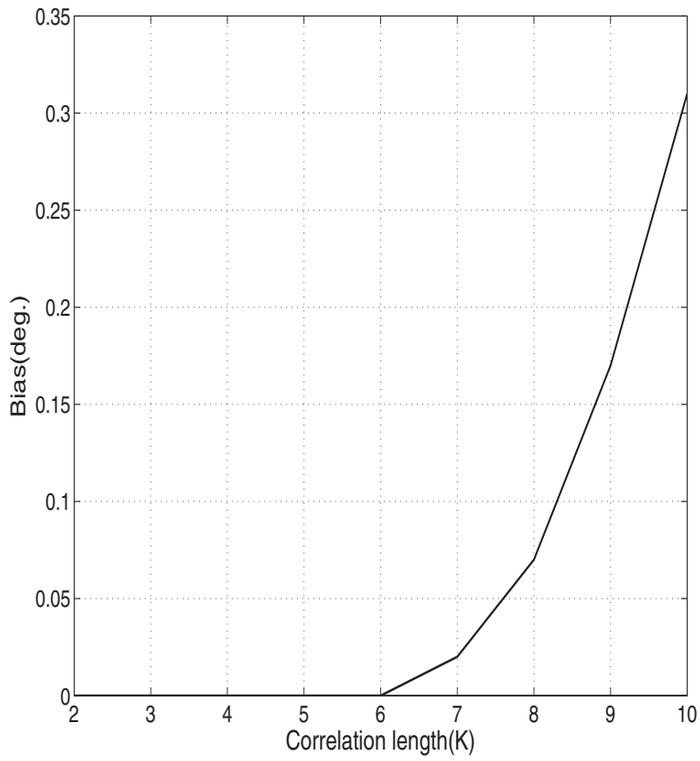

Fig. 12. Bias of the estimated direction according to spatial correlation length of the noise.

efficiency and the speed also depend on the signal-to-noise ratio, the number of sensors, the number of sources to be localized and the angular difference between the sources.

The spatial correlation length K authorized by the algorithm is a function of the number of sensors and the number of sources. Indeed, the number of parameters of the signal to be estimated is P^2 and the number of parameters of the noise is $Nber(K)$. In order to estimate them it is necessary that $N^2 \geq P^2 + Nber(K)$ and that $K \leq N$. In the limit case: $P = N - 1$, we have $Nber(K) \leq 2N - 1$, which corresponds to a bi-diagonal noise covariance matrix. If the model of the noise covariance matrix is band-Toeplitz (Tayem et al., 2006; Werner & Jansson, 2007), the convergence of the proposed algorithm is fast, and the correlation length of noise can reach N.

7. Experimental data

The studied signals are recorded during an underwater acoustic experiment. The experiment is carried out in an acoustic tank under conditions which are similar to those in a marine environment. The bottom of the tank is filled with sand. The experimental device is presented in figure 14. A source emits a narrow-band signal ($f_o = 350\ KHz$). In addition to the signal source a spatially correlated Gaussian noise is emitted. The signal-to-noise ratio is 5 dB. Our objective is to estimate the directions of arrival of the signals during the experiment. The signals are received on one uniform linear array. The observed signals come from various reflections on the objects being in the tank. Generally the aims of acousticians is the detection,

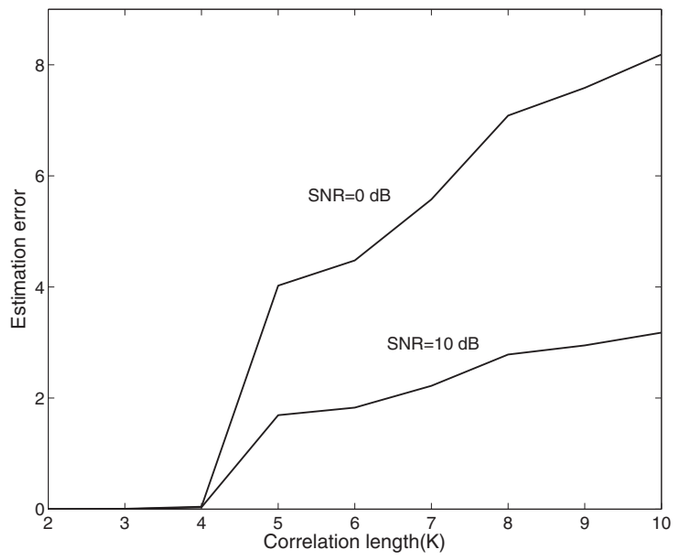

Fig. 13. Estimation error of the covariance matrix of the noise according to the spatial correlation length K and the signal-to-noise ratio SNR.

localization and identification of these objects. In this experiment we have recorded the reflected signals by a single receiver. This receiver is moved along a straight line between position $X_{min} = 50mm$ and position $X_{max} = 150mm$ with a step of α= $1mm$ in order to create a uniform linear array (see figure 15).

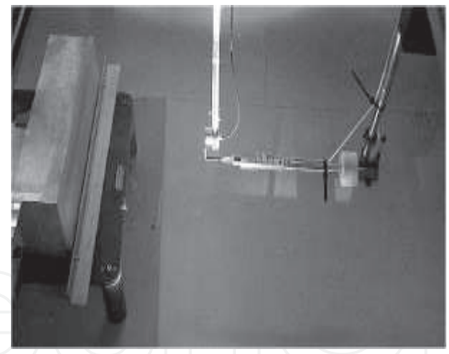

Fig. 14. Experimental device.

Two objects are placed at the bottom of the tank and the emitting source describes a circular motion with a step of 0.5° by covering the angular band going from 1° to 8.5°. The signals received when the angle of emission is θ=5° are shown in figure 16. This figure shows that there exists two paths, which may correspond to the reflected signals on the two objects. The results of the localization are given in figures 17 and 18. We note that in spite of the presence of the correlated noise our algorithm estimate efficiently the DOA of the reflected signals during the experiment.

Figure 17 shows the obtained results of the localization using MUSIC method on the covariance matrices. The DOA of the reflected signals on the two objects are not estimated. This is due to the fact that the noise is correlated.

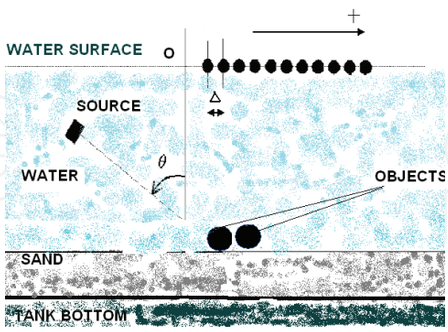

Fig. 15. Experimental setup.

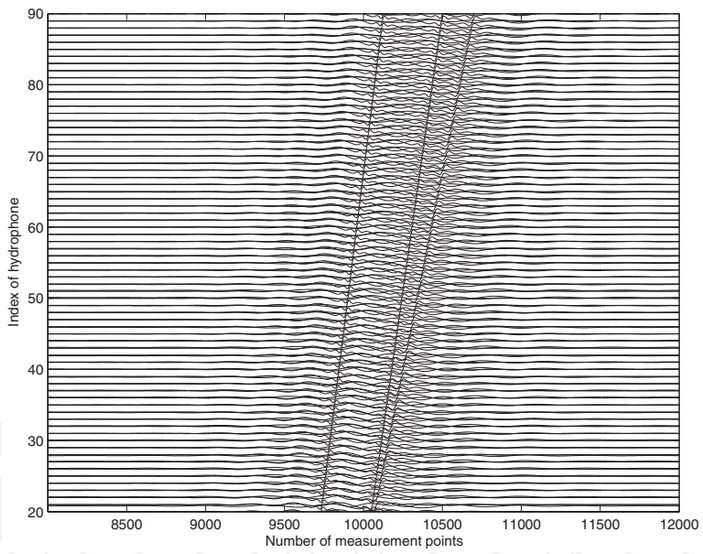

Fig. 16. Received signals.

Figure 18 shows the obtained results using our algorithm. The two objects are localized.

8. Cumulant based coherent signal subspace method for bearing and range estimation in noisy environment

In the rest of this chapter, we consider an array of N sensors which received the signals emitted by P wide band sources ($N > P$) in the presence of an additive Gaussian noise. The received signal vector, in the frequency domain, is given by

$$\mathbf{r}(f_n) = \mathbf{A}(f_n)\mathbf{s}(f_n) + \mathbf{n}(f_n), \quad \text{for} \quad n = 1, ..., M \tag{6}$$

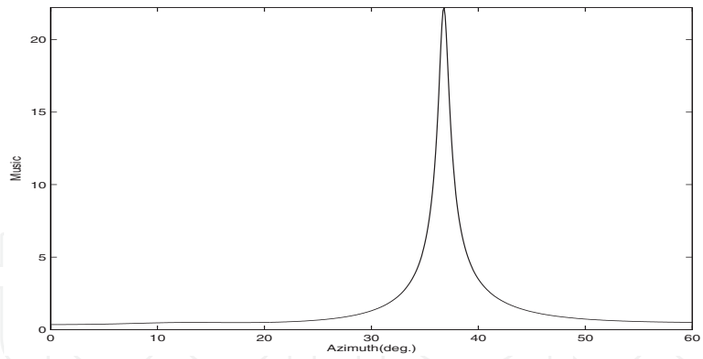

Fig. 17. Localization results with MUSIC.

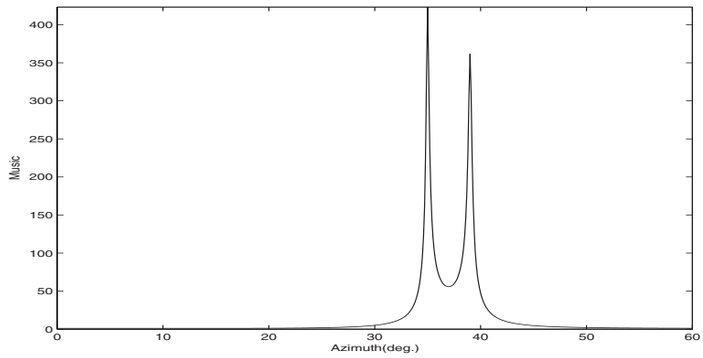

Fig. 18. Localization results with proposed algorithm.

where $\mathbf{A}(f_n) = [\mathbf{a}(f_n,\theta_1),\mathbf{a}(f_n,\theta_2),...,\mathbf{a}(f_n,\theta_P)]$, $\mathbf{s}(f_n) = [s_1(f_n),s_2(f_n),...,s_P(f_n)]^T$, and $\mathbf{n}(f_n) = [n_1(f_n),n_2(f_n),...,n_N(f_n)]^T$.
$\mathbf{r}(f_n)$ is the Fourier transforms of the array output vector, $\mathbf{s}(f_n)$ is the vector of zero-mean complex random non-Gaussian source signals, assumed to be stationary over the observation interval, $\mathbf{n}(f_n)$ is the vector of zero-mean complex white Gaussian noise and statistically independent of signals and $\mathbf{A}(f_n)$ is the transfer matrix (steering matrix) of the source sensor array systems computed by the $\mathbf{a}_k(f_n)$ $(k = 1,...,P)$ source steering vectors, assumed to have full column rank. In addition to the model (6), we also assume that the signals are statistically independent. In this case, a fourth order cumulant is given by

$$\begin{aligned}\mathrm{Cum}(r_{k_1},r_{k_2},r_{l_1},r_{l_2}) =& \mathrm{E}\{r_{k_1}r_{k_2}r_{l_1}^*r_{l_2}^*\} - \mathrm{E}\{r_{k_1}r_{l_1}^*\}\mathrm{E}\{r_{k_2}r_{l_2}^*\} \\ & - \mathrm{E}\{r_{k_1}r_{l_2}^*\}\mathrm{E}\{r_{k_2}r_{l_1}^*\}\end{aligned} \tag{7}$$

where r_{k_1} is the k_1 element in the vector $\mathbf{r}$ The indices k_2, l_1, l_2 are similarly defined. The cumulant matrix consisting of all possible permutations of the four indices $\{k_1,k_2,l_1,l_2\}$ is given in (Yuen & Friedlander, 1997) as

$$\mathbf{C}_g(f_n) \stackrel{\triangle}{=} \sum_{g=1}^{P}\Big(\mathbf{a}_g(f_n)\otimes\mathbf{a}_g^*(f_n)\Big)u_g(f_n)\Big(\mathbf{a}_g(f_n)\otimes\mathbf{a}_g^*(f_n)\Big)^+ \tag{8}$$

where $u_g(f_n)$ is the source kurtosis (i.e., fourth order analog of variance) defined by $u_g(f_n) = \mathrm{Cum}\big(s_g(f_n),s_g^*(f_n),s_g(f_n),s_g^*(f_n)\big)$ of the gth complex amplitude source and $\otimes$ is the Kronecker product, $\mathrm{Cum}(.)$ denotes the cumulant.

When there are N array sensors, $\mathbf{C}_g(f_n)$ is $(N^2 \times N^2)$ matrix. The rows of $\mathbf{C}_g(f_n)$ are indexed by $(k_1-1)N+l_1$, and the columns are indexed by $(l_2-1)N+k_2$. In terms of the vector $\mathbf{r}(f_n)$, the cumulant matrix $\mathbf{C}_g(f_n)$ is organized compatibly with the matrix $\mathrm{E}\{\big(\mathbf{r}(f_n)\otimes\mathbf{r}^*(f_n)\big)\big(\mathbf{r}(f_n)\otimes\mathbf{r}^*(f_n)\big)^+\}$. In other words, the elements of $\mathbf{C}_g(f_n)$ are given by $\mathbf{C}_g\big((k_1-1)N+l_1,(l_2-1)N+k_2\big)$ for $k_1,k_2,l_1,l_2=1,2,...,N$ and

$$\mathbf{C}_g\big((k_1-1)N+l_1,(l_2-1)N+k_2\big)=\mathrm{Cum}(r_{k_1},r_{k_2},r_{l_1},r_{l_2}) \tag{9}$$

where r_i is the ith element of the vector $\mathbf{r}$. In order to reduce the calculating time, instead of using of the cumulant matrix $(N^2\times N^2)$ $\mathbf{C}_g(f_n)$, a cumulant slice matrix $(N\times N)$ of the observation vector at frequency f_n can be calculated and it offers the same algebraic properties of $\mathbf{C}_g(f_n)$. This matrix is denoted $\mathbf{C}_1(f_n)$. If we consider a cumulant slice, for example, by using the first row of $\mathbf{C}_g(f_n)$ and reshape it into an $(N\times N)$ hermitian matrix, i.e.

$$\begin{aligned}\mathbf{C}_1(f_n)&\triangleq\mathrm{Cum}\big(r_1(f_n),r_1^*(f_n),\mathbf{r}(f_n),\mathbf{r}^+(f_n)\big)\\&=\begin{bmatrix}c_{1,1} & c_{1,N+1} & \cdots & c_{1,N^2-N+1}\\ c_{1,2} & c_{1,N+2} & \cdots & c_{1,N^2-N+2}\\ \vdots & \vdots & \vdots & \vdots\\ c_{1,N} & c_{1,2N} & \cdots & c_{1,N^2}\end{bmatrix}\end{aligned}$$

$$=\mathbf{A}(f_n)\mathbf{U}_s(f_n)\mathbf{A}^+(f_n) \tag{10}$$

where $c_{1,j}$ is the $(1,j)$ element of the cumulant matrix $\mathbf{C}_g(f_n)$ and $\mathbf{U}_s(f_n)$ is the diagonal kurtosis matrix, its ith element is defined as $\mathrm{Cum}\big(s_i(f_n),s_i^*(f_n),s_i(f_n),s_i^*(f_n)\big)$ with $i=1,...,P$.

$\mathbf{C}_1(f_n)$ can be reported as the classical covariance or spectral matrix of received data

$$\mathbf{\Gamma}_r(f_n)=\mathrm{E}\big[\mathbf{r}(f_n)\mathbf{r}^+(f_n)\big]=\mathbf{A}(f_n)\mathbf{\Gamma}_\mathbf{s}(f_n)\mathbf{A}^+(f_n)+\mathbf{\Gamma}_\mathbf{n}(f_n) \tag{11}$$

where $\mathbf{\Gamma}_n(f_n)=\mathrm{E}\big[\mathbf{n}(f_n)\mathbf{n}^+(f_n)\big]$ is the spectral matrix of the noise vector and $\mathbf{\Gamma}_s(f_n)=\mathrm{E}\big[\mathbf{s}(f_n)\mathbf{s}^+(f_n)\big]$ is the spectral matrix of the complex amplitudes $\mathbf{s}(f_n)$.
If the noise is white then: $\Gamma_n(f_n)=\sigma_n^2(f_n)\mathbf{I}$, where $\sigma_n^2(f_n)$ is the noise power and $\mathbf{I}$ is the $(N\times N)$ identity matrix. The signal subspace is shown to be spanned by the P eigenvectors corresponding to P largest eigenvalues of the data spectral matrix $\Gamma_r(f_n)$. But in practice, the noise is not often white or its spatial structure is unknown, hence the interest of the high order statistics as shown in equation (10) in which the fourth order cumulants are not affected by additive Gaussian noise (i.e., $\Gamma_n(f_n)=\mathbf{0}$), so as no noise spatial structure assumption is necessary. If the eigenvalues and the corresponding eigenvectors of $\mathbf{C_1}(\mathbf{f_n})$ are denoted by $\{\lambda_i(f_n)\}_{i=1..N}$ and $\{\mathbf{v_i}(\mathbf{f_n})\}_{\mathbf{i=1..N}}$. Then, the eigendecomposition of the cumulant matrix $\mathbf{C_1}(\mathbf{f_n})$ is exploited so as

$$\mathbf{C_1}(\mathbf{f_n})=\sum_{i=1}^{N}\lambda_i(f_n)\mathbf{v_i}(\mathbf{f_n})\mathbf{v_i^+}(\mathbf{f_n}) \tag{12}$$

In matrix representation, equation (12) can be written

$$\mathbf{C}_1(f_n)=\mathbf{V}(f_n)\mathbf{\Lambda}(f_n)\mathbf{V}^+(f_n) \tag{13}$$

where $\mathbf{V}(f_n) = [\mathbf{v}_1(f_n), ..., \mathbf{v}_N(f_n)]$ and $\mathbf{\Lambda}(f_n) = diag(\lambda_1(f_n), ..., \lambda_N(f_n))$.

Assuming that the columns of $\mathbf{A}(f_n)$ are all different and linearly independent it follows that for nonsingular $\mathbf{C}_1(f_n)$, the rank of $\mathbf{A}(f_n)\mathbf{U}_s(f_n)\mathbf{A}^+(f_n)$ is P. This rank property implies that:

- the $(N-P)$ multiplicity of its smallest eigenvalues : $\lambda_{P+1}(f_n) = \ldots = \lambda_N(f_n) \cong 0$.

- the eigenvectors corresponding to the minimal eigenvalues are orthogonal to the columns of the matrix $\mathbf{A}(f_n)$, namely, the steering vectors of the signals

$$\mathbf{V}_n(f_n) \stackrel{\triangle}{=} \{\mathbf{v}_{P+1}(f_n) \ldots \mathbf{v}_N(f_n)\} \perp \{\mathbf{a}(\theta_1, f_n) \ldots \mathbf{a}(\theta_P, f_n)\} \tag{14}$$

The eigenstructure based techniques are based on the exploitation of these properties. Then the directions of arrival of the sources are obtained, at the frequency f_n, by the peak positions in a so-called spatial spectrum (MUSIC)

$$\mathbf{Z}(f_n, \theta) = \frac{1}{\mathbf{a}^+(f_n, \theta)\mathbf{V}_n(f_n)\mathbf{V}_n^+(f_n)\mathbf{a}(f_n, \theta)} \tag{15}$$

For locating the wide band sources several solutions have been proposed in literature and are regrouped in this chapter into two groups:

- the incoherent subspace method: the analysis band is divided into several frequency bins and then at each frequency any narrow-band source localization algorithm can be applied and the obtained results are combined to obtain the final result. In addition of a significant calculating time, these methods do not carry out an actual wide band processing, but integrating information as well as possible coming from the various frequencies available to carry out the localization. It follows, for example, that the treatment gain does not increase with the analysis bandwidth. Indeed, it depends only on the resolving power narrow band processing for each considered frequency bin separately

- the coherent subspace method: the different subspaces are transformed in a predefined subspace using the focusing matrices (Valaee & Kabal, 1995; Hung & Kaveh, 1988). Then the obtained subspace is used to estimate the source parameters.

In the following section, the coherent subspace methods are described.

9. Coherent subspace methods

In the high resolution algorithm, the signal subspace is defined as the column span of the steering matrix $\mathbf{A}(f_n)$ which is function of the frequency f_n and the angles-of-arrival. Thus, the signal subspaces at different frequency bins are different. The coherent subspace methods (Hung & Kaveh, 1988) combine the different subspaces in the analysis band by the use of the focusing matrices. The focusing matrices $\mathbf{T}(\mathbf{f_o}, \mathbf{f_n})$ compensate the variations of the transfer matrix with the frequency. So these matrices verify

$$\mathbf{T}(f_o, f_n)\mathbf{A}(f_n) = \mathbf{A}(f_o), \quad for \quad n = 1, \ldots, M \tag{16}$$

where f_o is the focusing frequency.

Initially, Hung et al. (Hung & Kaveh, 1988) have developed the solutions for equation (16), the proposed solution under constraint $\mathbf{T}(f_o, f_n)\mathbf{T}^+(f_o, f_n) = \mathbf{I}$, is

$$\hat{\mathbf{T}}(f_o, f_n) = \mathbf{V}_l(f_o, f_n)\mathbf{V}_r^+(f_o, f_n) \tag{17}$$

where the columns of $\mathbf{V}_l(f_o, f_n)$ and of $\mathbf{V}_r(f_o, f_n)$ are the left and right singular vectors of the matrix $\mathbf{A}(f_n, \theta_i)\mathbf{A}^+(f_o, \theta_i)$ where θ_i is an initial vector of the estimates of the angles-of-arrival, given by an ordinary beamforming preprocess.

It has been shown that the performances of these methods depend on θ_i (Bourennane et al., 1997). In practice, it is very difficult to obtain the accurate estimate of the DOAs. So in order to resolve this initialization problem, the Two-Sided Correlation Transformation (TCT) algorithm is proposed in (Valaee & Kabal, 1995). The focusing matrices $\mathbf{T}(f_o, f_n)$ are obtained by minimizing

$$\begin{cases} \underset{\mathbf{T}(f_o,f_n)}{min} \|\mathbf{P}(f_o) - \mathbf{T}(f_o, f_n)\mathbf{P}(f_n)\mathbf{T}^+(f_o, f_n)\|_F \\ s.t \quad \mathbf{T}^+(f_o, f_n)\mathbf{T}(f_o, f_n) = \mathbf{I} \end{cases}$$

where $\mathbf{P}(.)$ is the array spectral matrix in noise free environment,
$\mathbf{P}(.) = \mathbf{A}(.)\Gamma_s(.)\mathbf{A}^+(.)$ and $\|.\|_F$ is the Frobenius matrix norm. The solution (Valaee & Kabal, 1995)is

$$\mathbf{T}(f_o, f_n) = \mathbf{V}(f_o)\mathbf{V}^+(f_n) \tag{18}$$

where $\mathbf{V}(f_o)$ and $\mathbf{V}(f_n)$ are the eigenvector matrices of $\mathbf{P}(f_o)$ and $\mathbf{P}(f_n)$, respectively.

In order to reduce the calculating time for constructing this operator equation (18), an improved solution is developed in (Bendjama et al., 1998), where only the signal subspace is used, however

$$\mathbf{T}(f_o, f_n)\mathbf{V}_s(f_n) = \mathbf{V}_s^+(f_o) \tag{19}$$

so the operator becomes

$$\mathbf{T}(f_o, f_n) = \mathbf{V}_s(f_o)\mathbf{V}_s^+(f_n) \tag{20}$$

where $\mathbf{V}_s(f_n) = [\mathbf{v}_1(f_n), \mathbf{v}_2(f_n), ..., \mathbf{v}_P(f_n)]$ are the eigenvectors corresponding to P largest eigenvalues of the spectral matrix $\mathbf{\Gamma}_r(f_n)$.

Once $\mathbf{\Gamma}_r(f_n)$ and $\mathbf{T}(f_o, f_n), n = 1..., M$ are formed, the estimate of $\hat{\mathbf{\Gamma}}_r(f_o)$ can be written

$$\hat{\mathbf{\Gamma}}_r(f_o) = \frac{1}{M}\sum_{n=1}^{M} \mathbf{T}(f_o, f_n)\mathbf{\Gamma}_r(f_n)\mathbf{T}^+(f_o, f_n) \tag{21}$$

In particular case, when equation (20) is used

$$\begin{aligned} \hat{\mathbf{\Gamma}}_r(f_o) &= \frac{1}{M}\sum_{n=1}^{M} \mathbf{V}_s(f_o)\mathbf{\Lambda}_s(f_n)\mathbf{V}_s^+(f_o) \\ &= \mathbf{V}_s(f_o)\hat{\mathbf{\Lambda}}_s(f_o)\mathbf{V}_s^+(f_o) \end{aligned} \tag{22}$$

where $\hat{\mathbf{\Lambda}}_s(f_o) = \frac{1}{M}\sum_{n=1}^{M} \mathbf{\Lambda}_s(f_n)$ is the arithmetic mean of the largest eigenvalues of the spectral matrices $\mathbf{\Gamma}_r(f_n)$ $(n = 1, ..., M)$.

Note that, the number of sources, P, can be computed by the number of non-zero eigenvalues of $\hat{\mathbf{\Gamma}}_r(f_o)$.

The efficiency of the different focusing algorithms is depended on the prior knowledge of the noise. All the transform matrices solution of equation system (16) are obtained in the presence of white noise or with the known spatial correlation structure.

In practice, as in underwater acoustic this assumption is not fulfilled then the performances of the subspace algorithms are degraded. To improve these methods in noisy data cases, in this paper, an algorithm is proposed to remove the noises. The basic idea is based on the combination of the high order statistics of received data, the multidimensional filtering and the frequential smoothing for eliminating the noise contributions.

10. Cumulant based coherent signal subspace

The high order statistics of received data are used to eliminate the Gaussian noise. For this the cumulant slice matrix expression (10) is computed. Then the $(P \times N)$ matrix denoted $\mathbf{H}(f_n)$ is formed in order to transform the received data with an aim of obtaining a perfect orthogonalization and eliminate the orthogonal noise component.

$$\mathbf{H}(f_n) = \mathbf{\Lambda}_s(f_n)^{-1/2}\mathbf{V}_s^+(f_n) \tag{23}$$

where $\mathbf{V}_s(f_n)$ and $\mathbf{\Lambda}_s(f_n)$ are the P largest eigenvectors and the corresponding eigenvalues of the slice cumulant matrix $\mathbf{C}_1(f_n)$ respectively. We note that it is necessary that the eigenvalues in $\mathbf{\Lambda}_s(f_n)$ be distinct. This is the case when the source kurtosis are different. If they are not, then the proposed algorithm will not provide correct estimates of the subspace signal sources. The $(P \times 1)$ vector of the transformed received data is

$$\mathbf{r}_t(f_n) = \mathbf{H}(f_n)\mathbf{r}(f_n) = \mathbf{H}(f_n)\mathbf{A}(f_n)\mathbf{s}(f_n) + \mathbf{H}(f_n)\mathbf{n}(f_n) \tag{24}$$

Afterwards, the corresponding $P^2 \times P^2$ cumulant matrix can be expressed as

$$\begin{aligned}\mathbf{C}_t(f_n) =& \mathrm{Cum}\left(\mathbf{r}_t(f_n), \mathbf{r}_t^+(f_n), \mathbf{r}_t(f_n), \mathbf{r}_t^+(f_n)\right)\\ =& \Big((\mathbf{HA})(f_n) \otimes (\mathbf{HA})^*(f_n)\Big)\mathbf{U}_s(f_n)\Big((\mathbf{HA})(f_n) \otimes (\mathbf{HA})^*(f_n)\Big)^+\end{aligned} \tag{25}$$

Or

$$\mathbf{C}_t(f_n) = \underbrace{\Big(\mathbf{B}(f_n) \otimes \mathbf{B}^*(f_n)\Big)}_{=\mathbf{B}_\otimes(f_n)}\mathbf{U}_s(f_n)\Big(\mathbf{B}(f_n) \otimes \mathbf{B}^*(f_n)\Big)^+ \tag{26}$$

Using the property (Mendel, 1991)

$$\mathbf{WX} \otimes \mathbf{YZ} = (\mathbf{W} \otimes \mathbf{Y})(\mathbf{X} \otimes \mathbf{Z}) \tag{27}$$

We can show that

$$\begin{aligned}\mathbf{C}_t(f_n) =& \Big(\mathbf{H}(f_n) \otimes \mathbf{H}^*(f_n)\Big)\Big(\mathbf{A}(f_n) \otimes \mathbf{A}^*(f_n)\Big)\mathbf{U}_s(f_n)\\ & \Big(\mathbf{A}(f_n) \otimes \mathbf{A}^*(f_n)\Big)^+\Big(\mathbf{H}(f_n) \otimes \mathbf{H}^*(f_n)\Big)^+\\ =& \Big(\mathbf{H}(f_n) \otimes \mathbf{H}^*(f_n)\Big)\mathbf{A}_\otimes(f_n)\mathbf{U}_s(f_n)\mathbf{A}_\otimes^+(f_n)\Big(\mathbf{H}(f_n) \otimes \mathbf{H}^*(f_n)\Big)^+\end{aligned} \tag{28}$$

Using (26) and (28), we have

$$\mathbf{B}_\otimes(f_n) = \Big(\mathbf{H}(f_n) \otimes \mathbf{H}^*(f_n)\Big)\mathbf{A}_\otimes(f_n) \tag{29}$$

Using the eigenvectors focusing operator defined as

$$\mathbf{T}(f_o, f_n) = \mathbf{V}_{ts}(f_o)\mathbf{V}_{ts}^{+}(f_n) \tag{30}$$

where $\mathbf{V}_{ts}(.)$ are the eigenvectors of the largest eigenvalues of the cumulant matrix $\mathbf{C}_t(.)$. The average cumulant matrix is

$$\begin{aligned}\hat{\mathbf{C}}_t(f_o) &= \frac{1}{M}\sum_{n=1}^{M}\mathbf{T}(f_o, f_n)\mathbf{C}_t(f_n)\mathbf{T}^{+}(f_o, f_n) \\ &= \mathbf{V}_{ts}(f_o)\hat{\mathbf{\Lambda}}_{ts}(f_o)\mathbf{V}_{ts}^{+}(f_o)\end{aligned} \tag{31}$$

where $\hat{\mathbf{\Lambda}}_{ts}(f_o) = \frac{1}{M}\sum_{n=1}^{M}\mathbf{\Lambda}_{ts}(f_n)$ is the arithmetic mean of the first largest eigenvalues of the cumulant matrix $\mathbf{C}_t(f_n)$. It is easy to show that

$$\hat{\mathbf{C}}_t(f_o) = \mathbf{V}_{ts}(f_o)\hat{\mathbf{\Lambda}}_{ts}(f_o)\mathbf{V}_{ts}^{+}(f_o) = \mathbf{B}_{\otimes}(f_o)\hat{\mathbf{U}}_s(f_o)\mathbf{B}_{\otimes}^{+}(f_o) \tag{32}$$

where $\mathbf{B}_{\otimes}(f_o) \stackrel{\triangle}{=} \mathbf{T}(f_o, f_n)\mathbf{B}_{\otimes}(f_n)$ and $\hat{\mathbf{U}}_s(f_o) = \frac{1}{M}\sum_{n=1}^{M}\mathbf{U}_s(f_n)$.

Multiplying both sides by $\mathbf{B}_{\otimes}^{+}(f_o)$, we get

$$\mathbf{B}_{\otimes}^{+}(f_o)\hat{\mathbf{C}}_t(f_o) = \mathbf{B}_{\otimes}^{+}(f_o)\mathbf{B}_{\otimes}(f_o)\hat{\mathbf{U}}_s(f_o)\mathbf{B}_{\otimes}^{+}(f_o) \tag{33}$$

Because the columns of $\mathbf{B}_{\otimes}(f_o)$ are orthogonal and the sources are decorrelated, $\mathbf{B}_{\otimes}^{+}(f_o)\mathbf{B}_{\otimes}(f_o)\hat{\mathbf{U}}_s(f_o)$ is a diagonal matrix which we will denote by $\mathbf{D}(f_o)$, so that we have

$$\mathbf{B}_{\otimes}^{+}(f_o)\hat{\mathbf{C}}_t(f_o) = \mathbf{D}(f_o)\mathbf{B}_{\otimes}^{+}(f_o) \tag{34}$$

Or

$$\hat{\mathbf{C}}_t(f_o)\mathbf{B}_{\otimes}^{+}(f_o) = \mathbf{D}(f_o)\mathbf{B}_{\otimes}(f_o) \tag{35}$$

This equation tells us that the columns of $\mathbf{B}_{\otimes}(f_o)$ are the left eigenvectors of $\hat{\mathbf{C}}_t(f_o)$ corresponding to the eigenvalues on the diagonal of the matrix $\mathbf{D}(f_o)$: however, since $\hat{\mathbf{C}}_t(f_o)$ is Hermitian, they are also the (right) eigenvectors of $\hat{\mathbf{C}}_t(f_o)$. Furthermore, the columns of $\mathbf{V}_{ts}(f_o)$ are also eigenvectors of $\hat{\mathbf{C}}_t(f_o)$ corresponding to the same (non-zero) eigenvectors of the diagonal matrix $\hat{\mathbf{U}}_s(f_o)$. Given that the eigenvalues of $\hat{\mathbf{C}}_t(f_o)$ are different, the orthonormal eigenvectors are unique up to phase term, this will likely be the case if the source kurtosis are different. Hence the difference between $\mathbf{V}_{ts}(f_o)$ and $\mathbf{B}_{\otimes}(f_o)$ is that the columns may be reordered and each column is multiplied by a complex constant.

The information we want is $\mathbf{A}_{\otimes}(f_o)$, which is given by (29)

$$\mathbf{A}_{\otimes}(f_o) = \Big(\mathbf{H}(f_o) \otimes \mathbf{H}^{*}(f_o)\Big)^{\dagger}\mathbf{B}_{\otimes}(f_o) \tag{36}$$

with † denoting the pseudo-inverse of matrix. We do not have the matrix $\mathbf{B}_{\otimes}(f_o)$, but we have the matrix $\mathbf{V}_{ts}(f_o)$. Hence we can obtain a matrix $\mathbf{A}'_{\otimes}(f_o)$ such that

$$\mathbf{A}'_{\otimes}(f_o) = \Big(\mathbf{H}(f_o) \otimes \mathbf{H}^*(f_o)\Big)^{\dagger} \mathbf{V}_{ts}(f_o) \tag{37}$$

Furthermore, we obtain $\hat{\mathbf{A}}(f_o)$ by extracting out the first N rows and the first P columns of $\mathbf{A}'_{\otimes}(f_o)$. The estimate $\hat{\mathbf{A}}(f_o)$ will be permuted and scaled (column-wise) version of $\mathbf{A}(f_o)$.

This algorithm leads to the estimation of the transfer matrix without prior knowledge of the steering vector or the propagation model such as in the classical techniques.

Therefore, the present algorithm for locating the wide band acoustic sources in the presence of unknown noise can be formulated as the following sequence of steps:

1) Form $\mathbf{C}_1(f_n)$ equation (10) and perform its eigendecomposition;
2) Form $\mathbf{H}(f_n)$ equation (23) $n = 1, ..., M$;
3) Calculate $\mathbf{r}_t(f_n)$ equation (24);
4) Form $\mathbf{C}_t(f_n)$ equation (25) and perform its eigendecomposition;
5) Form $\mathbf{T}(f_o, f_n)$ equation (30) $n = 1, ..., M$;
6) Form $\hat{\mathbf{C}}_t(f_o)$ equation (31) and perform its eigendecomposition;
7) Determine $\mathbf{A}'_{\otimes}(f_o)$ equation (37) and $\hat{\mathbf{A}}(f_o)$.

Naturally one can use the high resolution algorithm to estimate the azimuths of the sources. The orthogonal projector $\mathbf{\Pi}(\mathbf{f_o})$ is

$$\mathbf{\Pi}(f_o) = \mathbf{I} - [\hat{\mathbf{A}}^+(f_o)\hat{\mathbf{A}}(f_o)]^{-1}\hat{\mathbf{A}}^+(f_o) \tag{38}$$

where $\mathbf{I}$ is the (N×N) identity matrix. Hence, the narrow band Music can be directly applied to estimate the DOA of wide band sources according to

$$Z(f_o, \theta) = \frac{1}{\mathbf{a}^+(f_o, \theta)\mathbf{\Pi}(f_o)\mathbf{a}(f_o, \theta)} \tag{39}$$

with $\theta \in [-\pi/2, \pi/2]$.

11. Numerical results

In the following simulations, a linear antenna of $N = 10$ equispaced sensors with equal interelement spacing $d = \frac{c}{2f_o}$ is used, where f_o is the mid band frequency and c is the velocity of propagation. Eight $(P = 8)$ wide band source signals arrive at directions : $\theta_1 = 2°, \theta_2 = 5°$, $\theta_3 = 10°$, $\theta_4 = 12°$, $\theta_5 = 30°$, $\theta_6 = 32°$ $\theta_7 = 40°$ and $\theta_8 = 42°$, are temporally stationary zero-mean band pass with the same central frequency $f_o = 110Hz$ and the same bandwidth $B = 40Hz$. The additive noise is uncorrelated with the signals. The Signal-to-Noise Ratio (SNR) is defined here as the ratio of the power of each source signal to the average power of the noise variances, equals on all examples to $SNR = 10dB$.

Experiment 1: Improvement of source localization

In order to point out the improvement of the localization of the sources based on the higher order statistics, our first experiment is carried out in the context of the presence of Gaussian noise. Figures 19 and 20 show the obtained localization results of the eight simulated sources. The number of the sources is taken equal to 8. We can conclude that the fourth order statistics

of the received data have improved the spatial resolution. Indeed, the eight sources are perfectly separated. This improvement is due to the fact that the noise is removed using the cumulants.

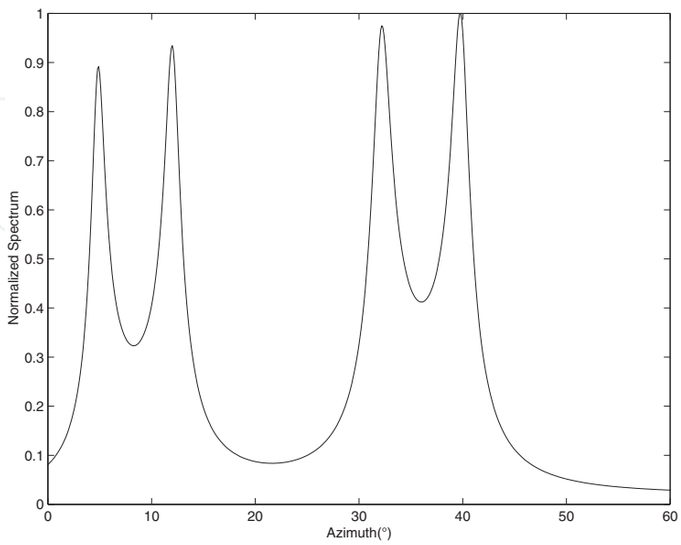

Fig. 19. Spectral matrix-Incoherent signal subspace, 8 uncorrelated sources.

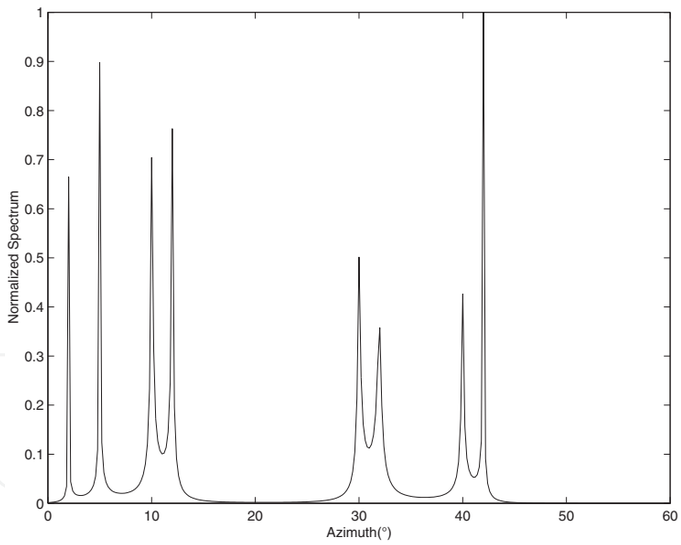

Fig. 20. Cumulant-Incoherent signal subspace, 8 uncorrelated sources.

Experiment 2: Localization of the correlated sources

The localization of a correlated sources is the delicate problem. The spatial smoothing is a solution (Pillai & Kwon, 1989), for the narrow band sources but limited to a linear antenna. In presence of white noise, it is well known that the frequential smoothing leads to localize the wide band correlated sources (Valaee & Kabal, 1995). In this experiment, the eight sources form two fully correlated groups in the presence of Gaussian noise with an unknown spectral matrix. Figures 21 and 22 give the source localization results, the obtained results show that

even the coherent signal subspace is used the performance of the high resolution algorithm is degraded (figure 21). Figure 22 shows the cumulant matrix improves the localization, this effectiveness is due to the fact that the noise contribution is null. It follows that the SNR after focusing is improved.

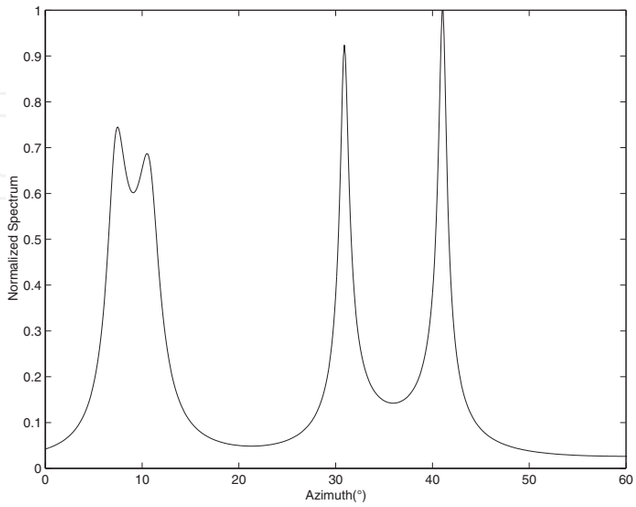

Fig. 21. Spectral matrix-Coherent signal subspace, two groups of correlated sources and Gaussian noise

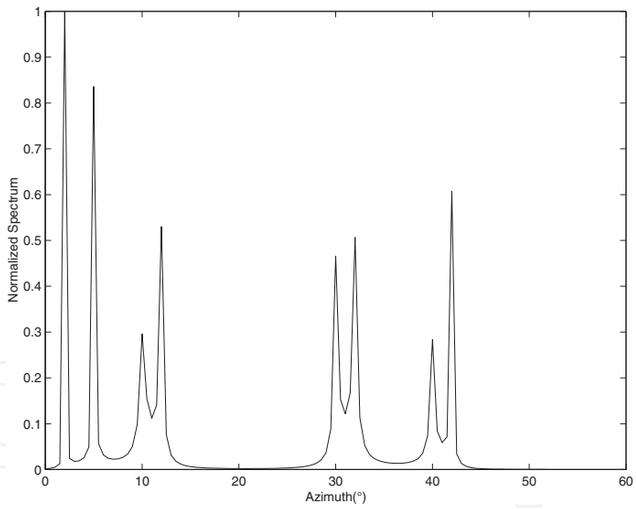

Fig. 22. Cumulant matrix-Coherent signal subspace, two groups of correlated sources and Gaussian noise

Experiment 3: Noise reduction- signal subspace projection

In this part, our algorithm is applied. The noise is modeled as the sum of Gaussian noise and spatially correlated noise. The eight sources are uncorrelated. Figure 23 shows that the cumulant matrix alone is not sufficient to localize the sources. But if the preprocessing of the received data is carried out by the projection of the data on the signal subspace to eliminate the components of the noise which is orthogonal to the signal sources, the DOA will be estimated as shown in figure 24.

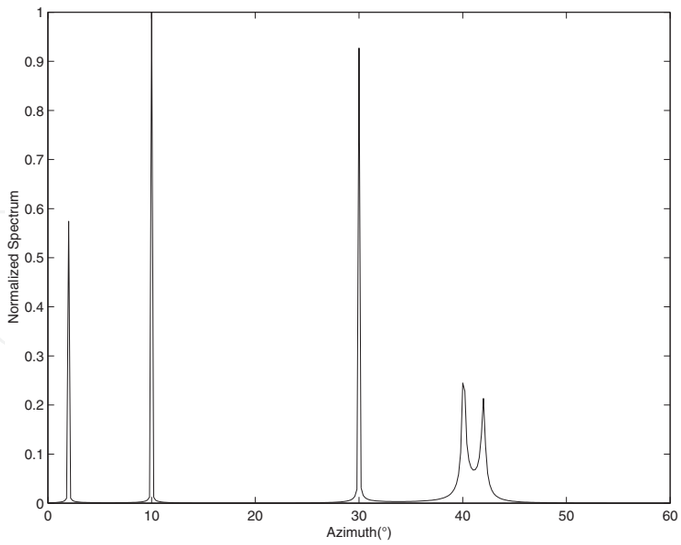

Fig. 23. Cumulant matrix incoherent signal subspace, 8 uncorrelated sources without whitening data

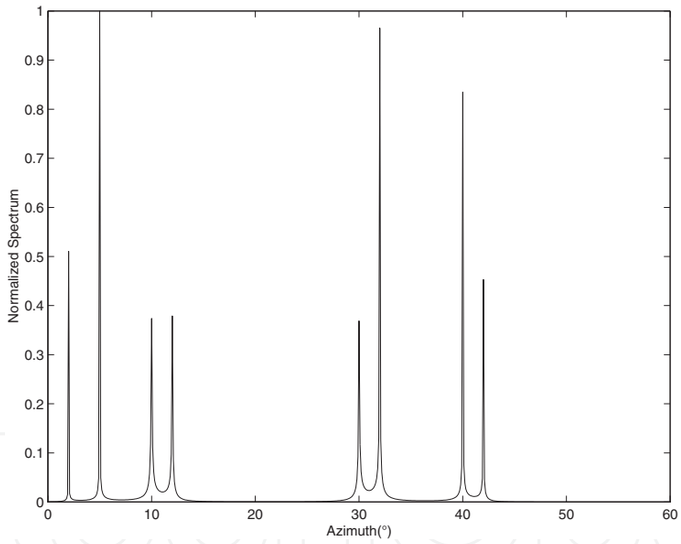

Fig. 24. Cumulant matrix incoherent signal subspace, 8 uncorrelated sources with whitening data

Figure 25 gives the obtained results with the coherent signal subspace when the sources are fully correlated. This last part points out the performance of our algorithm to localize the wide band correlated sources in the presence of unknown noise fields. Note that this results can be considered as an outstanding contribution of our study for locating the acoustic sources. Indeed, our algorithm allows to solve several practical problems. *Proposed algorithm performance:*

In order to study and to compare the performance of our algorithm to the classical wide band methods. For doing so, an experiment is carried out with the same former signals. Figure 26

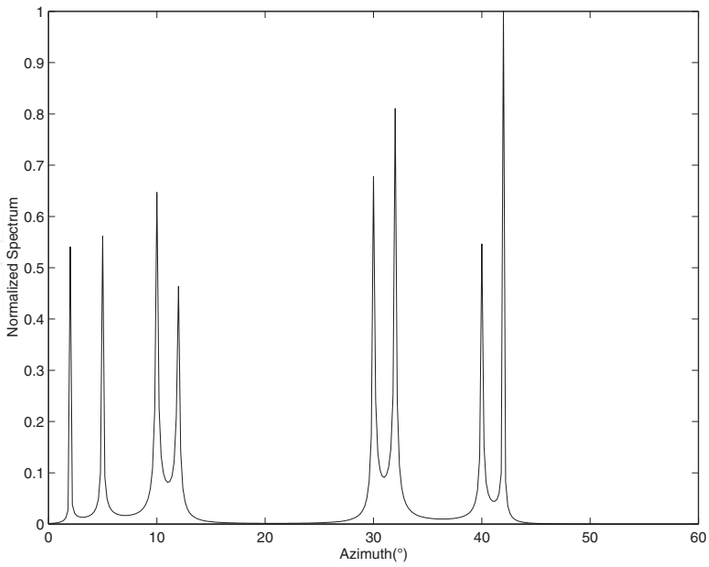

Fig. 25. Coherent cumulant matrices for two groups correlated sources after whitening data

shows the variation of the standard deviation (std) as function of SNR. The std is defined as $std = (1/k)[\sum_{i=1}^{k} |\hat{\theta}_i - \theta_i|^2]^{1/2}$, k is number of independent trials. The SNR is varied from $-40dB$ to $+40dB$ with $k = 500$ independent trials. One can remark the interest of the use of cumulant matrix instead of the spectral matrix and the improvement due to the whitening preprocessing or multidimensional filtering included in our algorithm. Our method after whitening presents the smallest std in all cases.

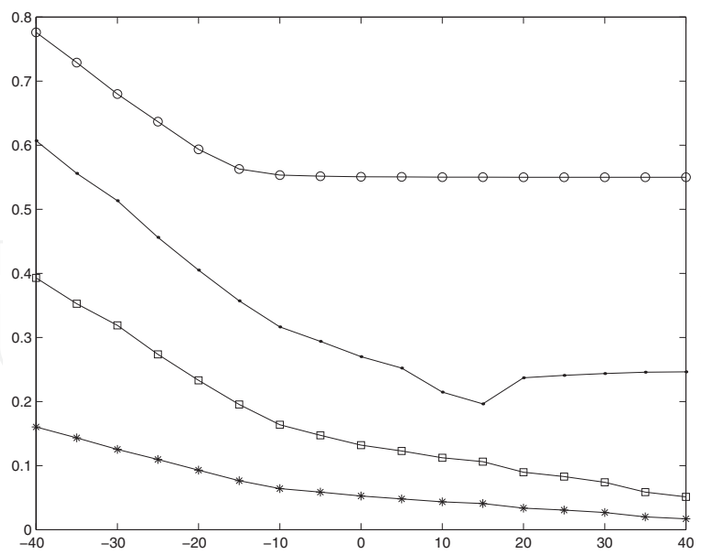

Fig. 26. Standard deviation comparison estimation: $-\circ$ Wang algorithm;

$-$. TCT algorithm; $-\square$ proposed method without whitening; $-*$ proposed method after whitening.

12. Conclusion

In this chapter the problem of estimating the direction-of-arrival (DOA) of the sources in the presence of spatially correlated noise is studied. The spatial covariance matrix of the noise is modeled as a band matrix and is supposed to have a certain structure. In the numerical example, the noise covariance matrix is supposed to be the same for all sources, which covers many practical cases where the sources are enclosed. This algorithm can be applied to the localization of the sources when the spatial-spectrum of the noise or the spatial correlation function between sensors is known. The obtained results show that the proposed algorithm improves the direction estimates compared to those given by the MUSIC algorithm without preprocessing. Several applications on synthetic data and experiment have been presented to show the limits of these estimators according to the signal-to-noise ratio, the spatial correlation length of the noise, the number of sources and the number of sensors of the array. The motivation of this work is to reduce the computational loads and to reduce the effect of the additive spatially correlated gaussian noise for estimating the DOA of the sources. We also presented methods to estimate the DOA algorithm for the wide band signals based on fourth order cumulants is presented. This algorithm is also applied to noisy data. Both the cumulants of the received data and multidimensional filtering processing are used to remove the additive noises. The principal interest of this preprocessing is the improvement of the signal to noise ratio at each analysis frequency. Then the signal subspace estimated from the average cumulant matrix resolves the fully correlated wide band acoustic sources. The simulation results are used to evaluate the performance and to compare the different coherent signal subspace algorithms. The obtained results show that the performances of the proposed algorithm are similar to those of the spectral matrix based methods when the noise is white and are better in the presence of Gaussian or an unknown noise. The Std variations and the localization results indicate that the whitening of the received data improves the localization in the presence of no completely Gaussian noise.

13. Acknowledgment

The authors would like to thank Dr Jean-Pierre SESSAREGO for providing real data and for his useful collaboration.

14. References

Reilly, J. & Wong, K. (1992). Estimation of the direction-of-arrival of signals in unknown correlated noise. Part II: Asymptotic behavior and performance of the MAP approach, *IEEE Trans. on signal processing*, Vol. 40, No. 8, (Aug. 1992) (2018-2028), ISSN 1053-587X .

Wu,Q. & Wong, K.(1994). UN-MUSIC and UN-CLE: An application of generated correlation analysis to the estimation of direction-of-arrival of signals in unknown correlated noise. *IEEE Trans. on signal processing*, Vol.42, No. 9, (1994) (2331-2343).

Stoica, P.; Vieberg, M. & Ottersten, B. (1994). Instrumental variable approach to array processing in spatially correlated noise fields. *IEEE Trans. on signal processing*, Vol.42, No. 1, (Jan. 1994) (121-133), ISSN 1053-587X .

Wax, M. (1991). Detection and localization of multiple sources in noise with known covariance. *IEEE Trans. on signal processing*, Vol. 40, No. 1, (Jan. 1992) (245-249), ISSN 1053-587X.

Ye, H. & De Groat, R. (1995). Maximum likelihood DOA estimation and asymptotic Cramer Rao Bounds for additive unknown colored noise. *IEEE on signal processing*, Vol. 43, No. 4, (Apr. 1995) (938-949), ISSN 1053-587X .

Zhang, Y. & Ye, Z. (2008). Efficient Method of DOA Estimation for Uncorrelated and Coherent Signals. *IEEE Antennas and Wireless Propagation Letters*, Vol. 7, (2008) (799-802), ISSN 1536-1225 .

Tayem, N.; Hyuck M. & Kwon. (2006). Azimuth and elevation angle estimation with no failure and no eigen decomposition. *EURASIP Signal Processing*, Vol. 86, No. 1, (2006) (8-16).

Cadzow, J.(1988). A high resolution direction-of-arrival algorithm for narrow-band coherent and incoherent sources. *IEEE Trans. on Acoustics, Speech and Signal Processing*, Vol. 36, No. 7, (1998) (965-979).

Werner, K. Jansson, M. (2007). DOA Estimation and Detection in Colored Noise Using Additional Noise-Only Data. *IEEE Trans. on signal processing*, Vol. 55, No. 11, (Nov. 2007) (5309-5322), ISSN 1053-587X .

Friedlander, B. & Weiss, A. (1995). Direction finding using noise covariance modeling. *IEEE Trans. on signal processing*, Vol. 43, No. 7, (Jul. 1995) (1557-1567), ISSN 1053-587X .

Abeidaa, H. & Delmas, P. (2007). Efficiency of subspace-based DOA estimators. *EURASIP Signal Processing*, Vol. 87, No. 9, (Sept. 2007) (2075-2084).

Kushki, A. & Plataniotis, K.N. (2009). Non parametric Techniques for Pedestrian Tracking in Wireless Local Area Networks. *Handbook on Array Processing and Sensor Networks* Haykin, S., Liu, K.J.R.,(Eds.), John Wiley & Sons, (783-803), ISBN 9780470371763

Hawkes, M. & Nehorai, A. (2001). Acoustic vector-sensor correlations in ambient noise. *IEEE J. Oceanic Eng.*, Vol. 26, No. 3, (Jul. 2001) (337-347).

Yuen, N. & Friedlander, B. (1997). DOA estimation in multipath : an approach using fourth order cumulants. *IEEE. Trans. on signal processing*, Vol. 45, No. 5, (May 1997) (1253-1263), ISSN 1053-587X .

Valaee, S. & Kabal, P. (1995). Wideband array processing using a two-sided correlation transformation. *IEEE Trans. on signal processing*, Vol. 43, No. 1, (Jan. 1995)(160-172), ISSN 1053-587X .

Hung, H. & Kaveh, M. (1988). Focusing matrices for coherent signal-subspace processing. *IEEE Trans. on Acoustics, Speech and Signal Processing*, Vol.36, No.8, (Aug. 1988) (1272-1281), ISSN 0096-3518 .

Bourennane, S.; Frikel M. & Bendjama, A. (1997). Fast wide band source separation based on higher order statistics. *Proceedings of IEEE Signal Processing Workshop on Higher Order Statistics*, pp.354-358, DOI 10.1109/HOST.1997.613546, Banff Canada, Jul. 1997.

Bendjama, A.; Bourennane, S. & Frikel, M. (1998). Direction Finding after Blind Identification of Source Steering Vectors. *Proceedings of SIP'98*, Las Vegas US, Oct. 1998.

Mendel, J.M. (1991). Tutorial on higher order statistics(spectra) in signal processing and system theory : Theoretical results and some applications. *IEEE Proceedings*, 1991, Vol.79, No.3, pp.278-305, March 1991.

Pillai S.& Kwon B. (1989). Forward/Backward spatial smoothing techniques for coherent signal identification. *IEEE Trans. on Acoustics, Speech and Signal Processing*, Vol.37, No.1, (jan. 1989)(8-15), ISSN 0096-3518 .

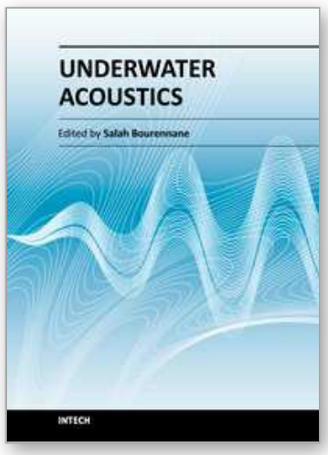

Underwater Acoustics

Edited by Prof. Salah Bourennane

ISBN 978-953-51-0441-4
Hard cover, 136 pages
Publisher InTech
Published online 28, March, 2012
Published in print edition March, 2012

How to reference

In order to correctly reference this scholarly work, feel free to copy and paste the following:

Salah Bourennane, Caroline Fossati and Julien Marot (2012). Array Processing: Underwater Acoustic Source Localization, Underwater Acoustics, Prof. Salah Bourennane (Ed.), ISBN: 978-953-51-0441-4, InTech, Available from: http://www.intechopen.com/books/underwater-acoustics/array-processing-underwater-acoustic-source-localization

INTECH
open science | open minds

InTech Europe
University Campus STeP Ri
Slavka Krautzeka 83/A
51000 Rijeka, Croatia
Phone: +385 (51) 770 447
Fax: +385 (51) 686 166
www.intechopen.com

InTech China
Unit 405, Office Block, Hotel Equatorial Shanghai
No.65, Yan An Road (West), Shanghai, 200040, China
中国上海市延安西路65号上海国际贵都大饭店办公楼405单元
Phone: +86-21-62489820
Fax: +86-21-62489821

IntechOpen